

## Adaptive Finite Element Method for Analysis of Pollutant Dispersion in Shallow Water

Somboon Otarawanna and Pramote Dechaumphai

Department of Mechanical Engineering, Faculty of Engineering, Chulalongkorn University, Bangkok 10330, Thailand.  
Tel: +66-(0)-2218-6621, Fax: +66-(0)-2252-2889, E-mail: fmepdc@eng.chula.ac.th

### Abstract

A finite element method for analysis of pollutant dispersion in shallow water is presented. The analysis is divided into two parts: (1) computation of the velocity flow field and the height of the water, and (2) computation of the pollutant concentration field from the dispersion model. The method is combined with an adaptive meshing technique to increase the solution accuracy, as well as to reduce the computational time and computer memory. The capability of the combined method is demonstrated by analyzing pollutant dispersion in Chaopraya river near the gulf of Thailand.

### 1. Introduction

Nowadays, both the industrial and urban zones in Thailand have increased rapidly. The discharge of thermally or chemically polluted water from power stations, industrial plants, and households into rivers has become threat to water resources. Authorities now require proof that the environmental impact of a planned discharge will not exceed a certain level, and plant designers must keep the impact below the specified level. For this reason, both authorities and plant designers have strong interest in reliable methods for predicting the distribution of pollutants resulting from a given discharge into a river.

The behavior of the pollutant dispersion in shallow water is governed by the conservation of mass and momentums, and the pollutant transport equation. The analysis may be considered as two-dimensional depth-averaged problem by assuming constant velocities over the depth with their values equal to the depth-averaged velocities. The above governing differential equations are coupled and nonlinear, and thus cannot be solved by analytical method especially for complex flow geometry. Several computational methods have been proposed in the past. These include the finite difference method [1-5], the finite volume

method [6-7] and the finite element method [8-12]. The finite element method is widely used currently because it can handle complex geometries effectively [12].

The accuracy of solution by the finite element method mainly depends on element sizes. High solution accuracy is obtained if small clustered elements are used in the model. However, the computational time and computer memory are increased if a large number of elements is used. Adaptive meshing technique [13-14] can be applied to increase the analysis solution accuracy, and to reduce the computational time and memory. The technique places small elements in the region of large change in the solution gradients to capture accurate solution, and at the same time, places larger elements in the other regions where the solutions are nearly uniform.

The paper starts by explaining the finite element formulation and the corresponding solution procedure that leads to the development of computer programs. The basic idea behind the adaptive meshing technique is then described. Finally, the efficiency of the combined method is demonstrated by example of pollutant dispersion in Chaopraya river.

### 2. The Flow Model

#### 2.1 Governing Equations

The governing equations that explain the flow behavior of shallow water flow can be derived by averaging the mass and momentum conservation equations in two-dimensional over the depth. These equations are [15],

$$\frac{\partial(Hu)}{\partial x} + \frac{\partial(Hv)}{\partial y} = 0 \quad (1a)$$

$$\left( u \frac{\partial u}{\partial x} + v \frac{\partial u}{\partial y} \right) = \left( \frac{\partial \sigma_x}{\partial x} + \frac{\partial \tau_{yx}}{\partial y} \right) - \frac{g\sqrt{u^2 + v^2}}{C^2 H} u \quad (1b)$$

$$\left( u \frac{\partial v}{\partial x} + v \frac{\partial v}{\partial y} \right) = \left( \frac{\partial \tau_{xy}}{\partial x} + \frac{\partial \sigma_y}{\partial y} \right) - \frac{g\sqrt{u^2 + v^2}}{C^2 H} v \quad (1c)$$

where  $H$  is the total water depth,  $u$  and  $v$  are the depth-averaged velocity components in  $x$  and  $y$  directions, respectively;  $g$  is the gravitational acceleration; and  $C$  is the Chezy friction coefficient. The stress components  $\sigma_x$ ,  $\sigma_y$ ,  $\tau_{xy}$  and  $\tau_{yx}$  are defined by,

$$\sigma_x = 2v \frac{\partial u}{\partial x} - g\zeta \quad (2a)$$

$$\sigma_y = 2v \frac{\partial v}{\partial y} - g\zeta \quad (2b)$$

$$\tau_{xy} = \tau_{yx} = v \left( \frac{\partial u}{\partial y} + \frac{\partial v}{\partial x} \right) \quad (2c)$$

and where  $\zeta$  is the elevation of the water surface over the mean surface level as shown in Fig. 1,  $\nu$  is the kinematics viscosity which can be written in form of the viscosity,  $\mu$ , and density,  $\rho$ , as

$$\nu = \frac{\mu}{\rho} \quad (3)$$

The differential equations, Eqs. (1a-c), are to be solved with appropriate boundary conditions which are either specifying depth-averaged velocity components along edge  $S_1$ ,

$$u = u_1(x, y) \quad (4a)$$

$$v = v_1(x, y) \quad (4b)$$

or surface tractions along edge  $S_2$ ,

$$T_x = \sigma_x \ell + \tau_{yx} m \quad (5a)$$

$$T_y = \tau_{xy} \ell + \sigma_y m \quad (5b)$$

where  $\ell$  and  $m$  are the direction cosines of the unit vector normal to the boundary edge.

## 2.2 Finite Element Formulation

The basic unknowns for the shallow water flow problem corresponding to the continuity equation (1a) and the two momentum equations (1b-c) are the depth-averaged velocity components  $u$ ,  $v$  and the water surface elevation  $\zeta$ . The six-node triangular element suggested in Ref. [16] is used in this

study. The element assumes quadratic interpolation for the velocity component distributions and linear interpolation for the water surface elevation distribution according to their highest derivative orders in the differential Eqs. (1a-c) as,

$$u(x, y) = N_\beta u_\beta \quad (6a)$$

$$v(x, y) = N_\beta v_\beta \quad (6b)$$

$$\zeta(x, y) = H_\mu \zeta_\mu \quad (6c)$$

where  $\beta = 1, 2, \dots, 6$ ;  $\mu = 1, 2, 3$ ;  $N_\beta$  and  $H_\mu$  are the element interpolation functions for the velocity and water surface elevation, respectively.

To derive the finite element equations, the method of weighted residuals [17] is applied to the momentum Eqs. (1b-c) and the continuity Eq. (1a),

$$\int_A N_i \left[ (uu_x + vv_y) - (\sigma_{xx} + \tau_{yx,y}) + \frac{g\sqrt{u^2 + v^2}}{C^2 H} u \right] dA = 0 \quad (7a)$$

$$\int_A N_i \left[ (uv_x + vv_y) - (\tau_{xy,x} + \sigma_{y,y}) + \frac{g\sqrt{u^2 + v^2}}{C^2 H} v \right] dA = 0 \quad (7b)$$

$$\int_A H_i [(Hu)_x + (Hv)_y] dA = 0 \quad (7c)$$

where  $A$  is the element area. Applying Gauss's theorem [17] to Eqs. (7a-b) for generating the element boundary integrals. That leads to the finite element equations which can be written in tensor form as,

$$K_{\alpha\beta\gamma} u_\beta u_\gamma + K_{\alpha\beta\gamma} v_\beta v_\gamma - H_{\alpha\mu} \zeta_\mu + S_{\alpha\beta} u_\beta + S_{\alpha\beta} v_\beta + C_{\alpha\beta} u_\beta = Q_{\alpha'} \quad (8a)$$

$$K_{\alpha\beta\gamma} u_\beta v_\gamma + K_{\alpha\beta\gamma} v_\beta v_\gamma - H_{\alpha\mu} \zeta_\mu + S_{\alpha\beta} u_\beta + S_{\alpha\beta} v_\beta + C_{\alpha\beta} v_\beta = Q_{\alpha'} \quad (8b)$$

$$J_{\mu\beta\eta} (\zeta_\mu + h_\mu) u_\beta + J_{\mu\beta\eta} (\zeta_\mu + h_\mu) v_\beta - R_{\eta\mu} \zeta_\mu = R_{\eta\mu} h_\mu \quad (8c)$$

where the coefficients in these equations are in form of the element interpolation functions.

The finite element equations, as shown in Eqs. (8a-c), are nonlinear to be solved by an iterative procedure. The Newton-Raphson iteration method is selected in this study. The method requires writing the unbalance values in the form,

$$F_{\alpha^*} = K_{\alpha\beta\gamma^*} u_{\beta} u_{\gamma} + K_{\alpha\beta\gamma^*} v_{\beta} u_{\gamma} - H_{\alpha\mu^*} \zeta_{\mu} + S_{\alpha\beta^*} u_{\beta} + S_{\alpha\beta^*} v_{\beta} + C_{\alpha\beta} u_{\beta} - Q_{\alpha^*} \quad (9a)$$

$$F_{\alpha^*} = K_{\alpha\beta\gamma^*} u_{\beta} v_{\gamma} + K_{\alpha\beta\gamma^*} v_{\beta} v_{\gamma} - H_{\alpha\mu^*} \zeta_{\mu} + S_{\alpha\beta^*} u_{\beta} + S_{\alpha\beta^*} v_{\beta} + C_{\alpha\beta} v_{\beta} - Q_{\alpha^*} \quad (9b)$$

$$F_{\eta} = J_{\mu\beta\eta^*} (\zeta_{\mu} + h_{\mu}) u_{\beta} + J_{\mu\beta\eta^*} (\zeta_{\mu} + h_{\mu}) v_{\beta} - R_{\eta\mu} (\zeta_{\mu} + h_{\mu}) \quad (9c)$$

Then application of the method leads to a set of algebraic equations with incremental unknowns in the form,

$$\begin{bmatrix} G_{\alpha\beta^*} & L_{\alpha\beta\gamma^*} & -H_{\alpha\mu^*} \\ L_{\alpha\beta^*} & G_{\alpha\beta\gamma^*} & -H_{\alpha\mu^*} \\ Z_{\eta\beta^*} & Z_{\eta\beta\gamma^*} & Q_{\eta\mu} \end{bmatrix} \begin{Bmatrix} \Delta u_{\beta} \\ \Delta v_{\beta} \\ \Delta \zeta_{\mu} \end{Bmatrix} = - \begin{Bmatrix} F_{\alpha^*} \\ F_{\alpha^*} \\ F_{\eta} \end{Bmatrix} \quad (10)$$

where the coefficients in the above equations are,

$$G_{\alpha\beta^*} = K_{\alpha\beta\gamma^*} u_{\gamma} + K_{\alpha\beta\gamma^*} v_{\gamma} + K_{\alpha\beta\gamma^*} v_{\gamma} + S_{\alpha\beta^*} + C_{\alpha\beta} \quad (11a)$$

$$G_{\alpha\beta^*} = K_{\alpha\beta\gamma^*} v_{\gamma} + K_{\alpha\beta\gamma^*} v_{\gamma} + K_{\alpha\beta\gamma^*} u_{\gamma} + S_{\alpha\beta^*} + C_{\alpha\beta} \quad (11b)$$

$$L_{\alpha\beta^*} = K_{\alpha\beta\gamma^*} v_{\gamma} + S_{\alpha\beta^*} \quad (11c)$$

$$L_{\alpha\beta^*} = K_{\alpha\beta\gamma^*} u_{\gamma} + S_{\alpha\beta^*} \quad (11d)$$

$$Z_{\eta\beta^*} = J_{\mu\beta\eta^*} (\zeta_{\mu} + h_{\mu}) \quad (11e)$$

$$Z_{\eta\beta^*} = J_{\mu\beta\eta^*} (\zeta_{\mu} + h_{\mu}) \quad (11f)$$

$$Q_{\eta\mu} = J_{\mu\beta\eta^*} u_{\beta} + J_{\mu\beta\eta^*} v_{\beta} - R_{\eta\mu} \quad (11g)$$

These coefficients which are in form of element matrices can be evaluated in closed-form for triangular elements ready for computer programming. Details of the derivation for these element matrices are omitted herein for brevity. In these Eqs. (11a-g),  $u_{\gamma}$  and  $v_{\gamma}$  are the values of the velocity components at the  $i^{\text{th}}$  iteration. The iteration process is terminated if the change in percentage of the overall errors of the nodal unknowns from the previous iteration is less than the specified value.

## 2.3 Adaptive Meshing Technique

The idea behind the adaptive meshing technique presented herein is to construct a new mesh based on the solution obtained from the previous mesh [14]. The new mesh consists of small elements in the regions with large change in solution gradients and larger elements in the regions where the change in solution gradients is small. For brevity, description of the adaptive meshing technique is omitted herein, but detail can be found in Refs. [14,17].

## 3. The Dispersion Model

### 3.1 Governing Equation

The depth-averaged pollutant transport equation is decoupled from the associated shallow water flow equations (1a-c) and is given by [15],

$$\frac{\partial(H\Theta)}{\partial t} + \frac{\partial(Hu\Theta)}{\partial x} + \frac{\partial(Hv\Theta)}{\partial y} = D \left[ \frac{\partial}{\partial x} \left( H \frac{\partial \Theta}{\partial x} \right) + \frac{\partial}{\partial y} \left( H \frac{\partial \Theta}{\partial y} \right) \right] \quad (12)$$

where  $\Theta$  is the pollutant concentration, and  $D$  is the dispersion coefficient. This differential equation is to be solved together with the boundary conditions that may consist of specifying the concentration,

$$\Theta = \Theta_1(x, y) \quad (13)$$

or its gradient,

$$\frac{\partial \Theta}{\partial n} = q_2(x, y) \quad (14)$$

and the initial condition of,

$$\Theta(x, y, 0) = \Theta_0 \quad (15)$$

### 3.2 Finite Element Formulation

The distribution for the element concentration is first assumed as,

$$\Theta(x, y, t) = \left[ N(x, y) \right]_{(1 \times 3)} \left\{ \Theta(t) \right\}_{(3 \times 1)} \quad (16)$$

where  $\left[ N(x, y) \right]_{(1 \times 3)}$  are the linear interpolation functions. Applying

the method of weighted residual and substituting Eq. (16) into Eq. (12) lead to the finite element equations in the form,

$$\begin{aligned} & \int_A \{W\} [N] dA \{\dot{\Theta}\} + \int_A \{W\} [u \quad v] [B] dA \{\Theta\} \\ & + \left\{ \int_A D \left( \left\{ \frac{\partial W}{\partial x} \right\} \left[ \frac{\partial N}{\partial x} \right] - \frac{1}{[N][H]} \{W\} \left[ \frac{\partial N}{\partial x} \right] \left[ \frac{\partial N}{\partial x} \right] \right) dA \right. \\ & \left. + \int_A D \left( \left\{ \frac{\partial W}{\partial y} \right\} \left[ \frac{\partial N}{\partial y} \right] - \frac{1}{[N][H]} \{W\} \left[ \frac{\partial N}{\partial y} \right] \left[ \frac{\partial N}{\partial y} \right] \right) dA \right\} \{\Theta\} \\ & = \int_s \{W\} q_n dS \quad (17) \end{aligned}$$

or,

$$[C]\{\dot{\Theta}\} + [K]\{\Theta\} = \{Q\} \quad (18)$$

### 3.3 Time Discretization

The explicit recurrence relations [17] are applied for time integration of Eq. (18). The application leads to,

$$\frac{1}{\Delta t} [C] \{\Theta\}_{n+1} = \left( \frac{1}{\Delta t} [C] + [K] \right) \{\Theta\}_n + \{Q\}_n \quad (19)$$

which can be solved directly for all nodal values of the pollutant concentration  $\Theta$  in the flow domain.

## 4. Application to Chaopraya River

### 4.1 Flow in the River

The geometry of the Chaopraya river is shown in Fig. 2. Figure 3 shows the finite element model and the boundary conditions with the inlet velocity of 1.5 m/s, kinematics viscosity  $\nu = 15 \text{ m}^2/\text{s}$ , Chezy coefficient  $C = 50\sqrt{\text{m}}/\text{s}$ , and the gravitational acceleration  $g = 9.81 \text{ m/s}^2$ . This initial finite element mesh consists of 4,111 nodes and 1,948 elements.

The numerical solution obtained from the initial mesh is then used to construct the second adaptive mesh as described in section 2.3. The second adaptive mesh consisting of 4,153 nodes and 1,954 elements is shown in Fig. 4. The figure shows smaller elements are generated in the regions where large change in velocity gradients occurs. At the same time, larger elements are generated in the other regions where the velocity is nearly uniform. With this second adaptive mesh, the entire procedure is repeated again to generate the third adaptive mesh with 3,411 nodes and 1,594 elements as shown in Fig. 5. The

corresponding flow solution and its detail are shown in Figs. 6 and 7, respectively.

### 4.2 Dispersion in the River

Contamination due to pollutant discharged from an industrial plant is studied. Figure 8 shows the boundary conditions with the initial condition of no pollutant concentration throughout the computational domain. The dispersion coefficient is given as  $83 \text{ m}^2/\text{s}$ . The final adaptive mesh of the flow model as shown in Fig. 5 is used as finite element mesh for the dispersion analysis. Figure 9 shows the computed concentration contours in the river at three hours after the plant disposal. Detail of distribution of pollutant concentration near the plant is also shown in Fig. 10.

## 5. Concluding Remarks

This paper presents the finite element method for analysis of pollutant dispersion in shallow water. The finite element formulation and its computational procedure is first described. The corresponding finite element equations are derived and the corresponding computer programs that can be executed on standard personal computer have been developed. The finite element method is combined with the adaptive meshing technique to improve the flow solution accuracy. The adaptive meshing technique generates an entirely new mesh based on the solution obtained from a previous mesh. The new mesh consists of clustered elements in the regions with large change in the velocity gradients to provide higher solution accuracy. At the same time, larger elements are generated in the other regions to reduce the computational time and computer memory. The results in this paper have demonstrated the capability of the combined method for the prediction of pollutant dispersion behaviors.

## 6. Acknowledgements

The authors are pleased to acknowledge the Thailand Research Fund (TRF), Bangkok, Thailand, for supporting this research work.

## References

- [1] Rastogi, A. K. and Rodi, W., "Predictions of Heat and Mass Transfer in Open Channels," *Journal of the Hydraulics Division*, Vol. 104, No. HY3, 1978, pp. 397-420.
- [2] Vreugdenhill, C. B. and Wijnnga, J. H., "A Computation of Flow Patterns in Rivers," *Journal of the Hydraulics Division*, Vol. 108, No. HY11, 1982, pp. 1296-1310.

[3] Demuran, A. O. and Rodi, W., "Calculation of Flow and Pollutant Dispersion in Meandering Channels," *Journal of Fluid Mechanics*, Vol. 172, 1986, pp. 63-92.

[4] Molls, T. and Chaudhry, M. H., "Depth-Averaged Open Channel Flow Model," *Journal of Hydraulic Engineering*, Vol. 121, No. 6, 1995, pp. 453-465.

[5] Borthwick, A. G. L. and Akponasa, G. A., "Reservoir Flow Prediction by Contravariant Shallow Water Equations," *Journal of Hydraulic Engineering*, Vol. 123, No. 5, 1997, pp. 432-439.

[6] Zhou, J. G. and Goodwill, I. M., "A Finite Volume Method for Steady State 2D Shallow Water Flows," *International Journal of Numerical Methods for Heat and Fluid Flow*, Vol. 7, No. 1, 1997, pp. 4-23.

[7] Yu, L. and Righetto, A. M., "Depth-Averaged Turbulence  $\tilde{k} - \tilde{\omega}$  Model and Applications," *Advances in Engineering Software*, Vol. 32, 2001, pp. 375-394.

[8] Zienkiewicz, O. C. and Heinrich, J. C., "A Unified Treatment of Steady-State Shallow Water and Two-Dimensional Navier-Stokes Equations-Finite Element Approach," *Computer Methods in Applied Mechanics and Engineering*, Vol. 17/18, 1979, pp. 673-698.

[9] Cochet, J. F., Dhatt, D., Hubert, G. and Touzot, G., "River and Estuary Flows by A New Penalty Finite Element," *Finite Element Flow Analysis*, Edited by Kawai, T., University of Tokyo Press, Tokyo, 1982, pp. 563-570.

[10] Leclerc, M., Bellemare, J., Dumas, G. and Dhatt, G., "A Finite Element Model of Estuarine and River Flows with Moving Boundaries," *Advances in Water Resources*, Vol. 13, No. 4, 1990, pp. 158-168.

[11] Shrestha, P. L., "An Integrated Model Suite for Sediment Pollutant Transport in Shallow Lakes," *Advances in Engineering Software*, Vol. 27, 1996, pp. 201-212.

[12] Tabuenca, P., Vila, J., Cardona, J. and Samartin, A., "Finite Element Simulation of Dispersion in The Bay of Santander," *Advances in Engineering Software*, Vol. 28, 1997, pp. 313-332.

[13] Peraire, J., Vahjdati, M., Morgan, K. and Zienkiewicz, O. C., "Adaptive Remeshing for Compressible Flow Computation," *Journal of Computational Physics*, Vol. 72, 1987, pp. 449-466.

[14] Dechaumphai, P., "Adaptive Finite Element Technique for Heat Transfer Problems," *Energy, Heat and Mass Transfer*, Vol. 17, 1995, pp. 87-94.

[15] Otarawanna, S., "Finite Element Method for Analysis of Pollutant Dispersion in Shallow Water," Master Thesis, Mechanical Engineering, Faculty of Engineering, Chulalongkorn University, 2002.

[16] Yamada, Y., Ito, K., Yokouchi, T., and Ohtsubo, T., "Finite Element Analysis of Steady Fluid and Metal Flow," *Finite Element in Fluid*, Edited by Gallagher, R. H., et al., John Wiley and Sons, New York, 1975.

[17] Dechaumphai, P., *Finite Element Method for Computational Fluid Dynamics*, Chulalongkorn University Press, Bangkok, 2002.

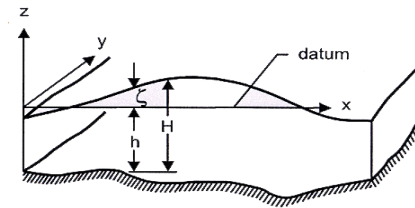


Fig. 1 – The notation of shallow water problem

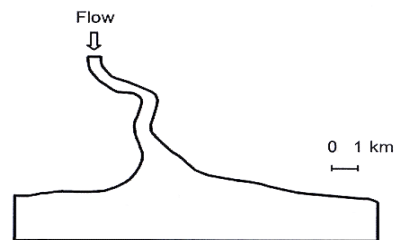


Fig. 2 – Computational domain of Chaopraya river

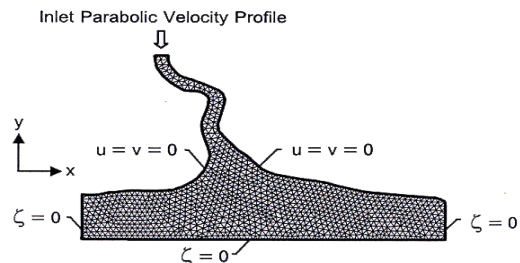


Fig. 3 – Initial finite element mesh and boundary conditions for flow in Chaopraya river

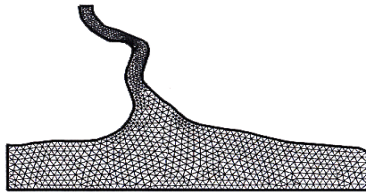


Fig. 4 – Second finite element mesh for flow in Chaopraya river

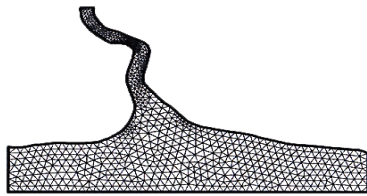


Fig. 5 – Third finite element mesh for flow in Chaopraya river

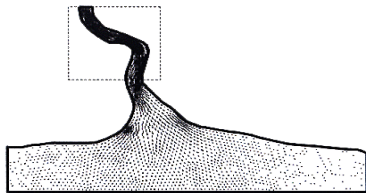


Fig. 6 – Predicted velocity distribution for flow in Chaopraya river

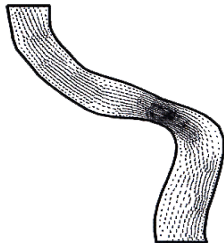


Fig. 7 – Detail of predicted velocity distribution for flow in Chaopraya river

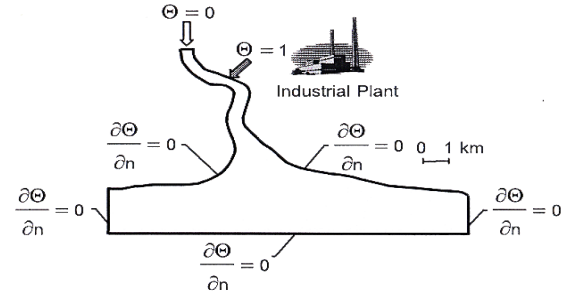


Fig. 8 – Computational domain and boundary conditions for pollutant dispersion in Chaopraya river



Fig. 9 – Predicted distribution of pollutant concentration for pollutant dispersion in Chaopraya river at three hours after the plant disposal

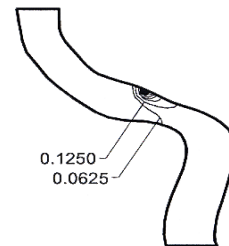


Fig. 10 – Detail of distribution of pollutant concentration for pollutant dispersion in Chaopraya river at three hours after the plant disposal